










**RESEARCH ARTICLE**

# Antimicrobial activity and cytotoxicity study of cerium oxide nanoparticles with two different sizes

Svetlana Yefimova<sup>1</sup>  | Vladimir Klochkov<sup>1</sup>  | Nataliya Kavok<sup>1</sup> |  
 Anton Tkachenko<sup>2</sup>  | Anatolii Onishchenko<sup>2</sup>  | Tatyana Chumachenko<sup>2,3</sup>  |  
 Nadir Dizge<sup>4</sup>  | Sadin Özdemir<sup>5</sup>  | Serpil Gonca<sup>6</sup>  | Kasim Ocakoglu<sup>7</sup> 

<sup>1</sup>Department of Nanostructured Materials, Institute for Scintillation Materials, National Academy of Sciences of Ukraine, Kharkiv, Ukraine

<sup>2</sup>Research Institute of Experimental and Clinical Medicine, Kharkiv National Medical University, Kharkiv, Ukraine

<sup>3</sup>Department of Epidemiology, Kharkiv National Medical University, Kharkiv, Ukraine

<sup>4</sup>Department of Environmental Engineering, Mersin University, Mersin, Turkey

<sup>5</sup>Food Processing Programme, Technical Science Vocational School, Mersin University, Mersin, Turkey

<sup>6</sup>Faculty of Pharmacy, Department of Pharmaceutical Microbiology, Mersin University, Mersin, Turkey

<sup>7</sup>Faculty of Engineering, Department of Engineering Fundamental Sciences, Tarsus University, Tarsus, Turkey

**Correspondence**

Anton Tkachenko, Research Institute of Experimental and Clinical Medicine, Kharkiv National Medical University, Nauky av 4, Kharkiv 61022, Ukraine.  
 Email: [as.tkachenko@knmu.edu.ua](mailto:as.tkachenko@knmu.edu.ua)

**Funding information**

National Research Foundation of Ukraine, Grant/Award Number: 0120U105451

**Abstract**

The control over bacterial diseases requires the development of novel antibacterial agents. The use of antibacterial nanomedicines is one of the strategies to tackle antibiotic resistance. The study was designed to assess the antimicrobial activity of cerium oxide (CeO<sub>2</sub>) nanoparticles (NP) of two different sizes (CeO<sub>2</sub> NP1 [1–2 nm] and CeO<sub>2</sub> NP2 [10–12 nm]) and their cytotoxicity towards eukaryotic cells. The antimicrobial activity, effects of nanoparticles on DNA cleavage, microbial cell viability, and biofilm formation inhibition were analyzed. The impact of cerium oxide nanoparticles on eryptosis of erythrocytes was estimated using annexin V staining by flow cytometry. The newly synthesized CeO<sub>2</sub> NP1 and CeO<sub>2</sub> NP2 displayed moderate antimicrobial activities. CeO<sub>2</sub> NP1 and CeO<sub>2</sub> NP2 exhibited single-strand DNA cleavage ability. CeO<sub>2</sub> NPs were found to show 100% microbial cell viability inhibition at a concentration of 500 mg/L. In addition, CeO<sub>2</sub> NP1 and CeO<sub>2</sub> NP2 inhibited the biofilm formation of *S. aureus* and *P. aeruginosa*. Larger cerium oxide nanoparticles were found to be less toxic against erythrocytes compared with the smaller ones. CeO<sub>2</sub> nanoparticles demonstrate moderate antimicrobial activity and low cytotoxicity towards erythrocytes, which make them promising antibacterial agents.

**KEYWORDS**

antimicrobial, biofilm inhibition, cerium, DNA cleavage, microbial cell viability, nanoparticle

**1 | INTRODUCTION**

Antibiotics have been used for decades to treat bacterial infections. Furthermore, they are widely used in agriculture and animal husbandry to prevent the emergence of infectious diseases in animals and increase overall productivity.<sup>1,2</sup> In addition to the widespread use of antibiotics, there are a lot of concerns over their misuse and overuse. The improper use of antibiotics, including their prescription for preventive purposes without the corresponding indications, has undermined the efficiency of these antimicrobial drugs and

promoted the emergence of an antibiotic resistance crisis.<sup>3</sup> The growing prevalence of antibiotic-resistant bacteria is a serious threat to national and international public health systems. Several approaches have been suggested to overcome or at least reduce the burden of bacterial infections caused by the resistant strains, including antimicrobial peptides, bacteriophages, targeting quorum sensing and biofilm formation, and so forth.<sup>4–8</sup> All of the strategies mentioned above have their advantages and disadvantages. However, despite the obvious achievements in developing antibacterial therapeutic agents alternative to antibiotics and even the promising

results of clinical trials, their implementation in clinical medicine is still of limited value.

Among the potential antibacterial therapeutic agents, nanoparticles (NPs), which are materials whose at least one dimension is 1–100 nm, have gained a lot of attention. The unique features of NPs make them promising candidates with high antimicrobial ability. For example, the large surface-to-volume ratio of NPs rises the interaction area with bacteria and allows their functionalization with ligands favoring contacts with microorganisms. In most cases, toxicity of NPs is attributed to the released metallic ions; the antimicrobial activity of NPs is extremely dependent on their physicochemical properties such as surface, size, and charge. Furthermore, these features can be engineered to maximize microorganism–NP contacts, biofilm penetration, and NP antimicrobial efficacy. Nanoparticle size is a significant factor as it determines whether NPs penetrate the microbial cells and biofilms, thus rising up their toxicity.<sup>9</sup> Given the mechanisms of antimicrobial activity typical for NPs (induction of oxidative stress, release of metal ions, DNA damage, ATP depletion, non-oxidative pathways such as changes at the transcriptomic, and proteomic levels), bacteria can develop the resistance to such agents to a lesser extent compared with conventional antibiotics.<sup>10,11</sup> However, a growing body of evidence suggests that bacteria develop some mechanisms to counteract silver NPs, including flagellin production to cause agglomeration of NPs, pigment synthesis to bind them or formation of efflux pumps to excrete NPs.<sup>12–14</sup> This suggests the requirements for developing alternative to silver antibacterial nanomaterials.

There is compelling evidence that metal-containing NPs (gold, silver, copper, their oxides, etc.) have strong bactericidal effects.<sup>15,16</sup> Several studies have demonstrated that cerium oxide (CeO<sub>2</sub>) NPs show antimicrobial effects.<sup>17–19</sup> Furthermore, it is worth noting that these nanomaterials have low toxicity against eukaryotic cells. However, the antimicrobial effects of metal-containing are known to be shape- and size-dependent.<sup>20</sup> Thus, it is important to compare the effects of CeO<sub>2</sub> NPs of various sizes on different bacterial strains.

The aim of this study was to assess the antibacterial potential of CeO<sub>2</sub> nanoparticles and evaluate their cytotoxicity against eukaryotic cells. CeO<sub>2</sub> NPs was synthesized with two different sizes (2 and 10 nm) and characterized by transmission electron microscopy (TEM) and X-ray diffraction spectra (XRD).

## 2 | MATERIALS AND METHODS

### 2.1 | CeO<sub>2</sub> NPs synthesis and characterization methods

Cerium oxide NPs of two sizes (~2 and 10 nm) were obtained in a form of aqueous colloidal solutions at a concentration of 1–2 mg/ml (pH = 7.2–7.8) by the method described earlier.<sup>21</sup> Briefly, 100 ml of 2 mM CeCl<sub>3</sub> (99%, Acros Organics) solution was mixed with 100 ml of 4 mM hexamethylenetetramine (HMTA, 99.2%, Acros Organics) and stirred using a magnetic stirrer for 3 h at room temperature. The size of obtained CeO<sub>2</sub> NPs was governed by the CeCl<sub>3</sub>:HMTA ratio. The CeCl<sub>3</sub>:HMTA = 1:1 gives the size of CeO<sub>2</sub> NPs of about 10 nm. The

excess of HMTA decreases the size of CeO<sub>2</sub> NPs down to 2 nm. After 3 h stirring, 1.8 ml NH<sub>4</sub>OH and 0.6 ml of H<sub>2</sub>O<sub>2</sub> were added into the solution and the solution was put into a round-bottom flask and refluxed for 5 h to obtain transparent colorless solutions. The mixture was evaporated in a rotary evaporator flask under vacuum at the bath temperature of 70°C to 30 ml adding 2 M NaCl until the resulting solution became turbid. Then the solid phase was precipitated by centrifugation. The precipitate was separated, and a solution of NaCl was added again. The procedure of precipitate cleaning was repeated three times. After the last stage of centrifugation, a solution of sodium citrate Na<sub>3</sub>C<sub>6</sub>H<sub>5</sub>O<sub>7</sub> (NaCt, 99%, Acros Organic) with molar ratio CeO<sub>2</sub>:NaCt = 1:1 was added to the precipitate for NPs stabilization. To remove the excess ions and organic impurities, the final solution was dialyzed for 24 h against deionized water. Dialysis membrane tubing with a molecular weight “Cellu Sep H1” 3.5 KDa cutoff (pore size of less than 1.5 nm) was used.

Transmission electron microscopy (TEM) images of as-synthesized CeO<sub>2</sub> NPs were obtained using a TEM-125 K electron microscope (Selmi, Ukraine) and a 90 kV electron beam. The samples were obtained by evaporation of droplets of diluted CeO<sub>2</sub> colloidal solutions placed on carbon-coated copper grids (200 Mesh, Electron Microscopy Sciences, USA). Zeta potentials of the CeO<sub>2</sub> NPs were measured using a ZetaPALS/BIMAS analyzer (Brookhaven Instruments Corp., USA) operated in the phase analysis light scattering mode.

X-ray diffraction spectra (XRD) of CeO<sub>2</sub> NPs were recorded using a Siemens D500 X-ray diffractometer (Germany).

### 2.2 | Analysis of CeO<sub>2</sub> NPs cytotoxicity against non-nucleated eukaryotic cells

Blood samples were collected from 6 intact WAG rats weighing 180–220 g in sterile K<sub>2</sub>EDTA Vacutainers (IMPROVACUTER Evacuated EDTA K<sub>2</sub> Spray Dried PET Tubes, Guangzhou, China). Blood aliquots were incubated horizontally with CeO<sub>2</sub> NPs (d = 2 and 10 nm) in PBS for 90 min at concentrations of 0, 50, 125, and 250 mg/L.

After incubation, blood was washed twice in PBS. Thereafter, 2 μl of erythrocytes were added to 100 μl 1× Annexin-binding buffer (BD Pharmingen™ Annexin V Binding Buffer, BD Biosciences, San Jose, USA) and incubated with 5 μl of fluorescein isothiocyanate (FITC)-labeled Annexin V (BD Pharmingen™FITC-Annexin V, BD Biosciences, San Jose, USA) for 30 min. Erythrocyte suspensions treated with H<sub>2</sub>O<sub>2</sub> (0.1 mM) were used as a positive control. Incubation was followed by the addition of 400 μl 1× Annexin-binding buffer to each sample.

Data were acquired by a FACS Canto II flow cytometer (BD, USA). Acquired data were analyzed using FlowJo™ (v10, BD Biosciences, USA).

### 2.3 | Antibacterial activity of CeO<sub>2</sub> NPs by using micro-dilution assay

Minimum inhibitory concentration (MIC) of synthesized CeO<sub>2</sub> NP1 and CeO<sub>2</sub> NP2 were investigated against *Enterococcus faecalis* (ATCC

29212), *Staphylococcus aureus* (ATCC 25923), *Pseudomonas aeruginosa* (ATCC 27853), *Enterococcus hirae* (ATCC 10541), *Legionella pneumophila subsp. pneumophila* (ATCC 33152), *Escherichia coli* (ATCC 25922), *Candida parapsilosis* (ATCC 22019), and *Candida tropicalis* (ATCC 750) by utilizing micro-dilution assay. The microbial cultures were incubated overnight before the micro-dilution assay. Two-fold serial dilutions of CeO<sub>2</sub> NP1 and CeO<sub>2</sub> NP2 were done and then the test microorganisms were added to the microplatewells. Next, plates were kept in an oven for 24 h incubation at 37°C. At the end of incubation, antimicrobial activity was evaluated by assessing MIC values, which are defined as the lowest concentration that prevented microbial growth.

## 2.4 | DNA cleavage ability

To investigate the DNA cleavage ability of synthesized CeO<sub>2</sub> NP1 and CeO<sub>2</sub> NP2, plasmid pBR322 DNA was used as the target DNA molecule. Initially, 0.1 mg/L DNA molecule was exposed to different levels of synthesized CeO<sub>2</sub>NPs at 37°C for 60 min. Then, the agarose gel electrophoresis method was used to visualize the DNA cleavage ability of the synthesized CeO<sub>2</sub>NPs. DNA bands were visualized using a transilluminator.

## 2.5 | Bacterial viability test

*E. coli* (ATCC 10536) was used to assess the impact of CeO<sub>2</sub>NPs on cell viability. After *E. coli* was inoculated into NB (Nutrient Broth) media, it was incubated for 24 h at 37°C at 150 rpm in a shaker. After 24 h, culture media were centrifuged at 5000 rpm for 5 min. *E. coli* pellet was then washed with sterile saline solution to remove fermentation media residual. The washed *E. coli* was suspended in NaCl solution. This *E. coli* suspension was used for evaluating microbial cell viability. *E. coli* was treated with 125, 250, and 500 mg/L of synthesized CeO<sub>2</sub>NPs for 90 min at 37°C. After 90 min, they were diluted in different proportions and inoculated in NB agar media and incubated at 37°C for 24 h. The same application was performed for the control group, which did not contain synthesized CeO<sub>2</sub> NPs. Finally, the colonies were counted and the microbial cell viability was calculated using Equation (1).

$$\text{Cell viability (\%)} = \left[ \frac{A_{\text{control}} - A_{\text{sample}}}{A_{\text{control}}} \right] \times 100 \quad (1)$$

## 2.6 | Biofilm inhibition activity

*S. aureus* and *P. aeruginosa* were used as test microorganisms for determining the impact of synthesized CeO<sub>2</sub>NPs on biofilm inhibition. Well plates containing various concentrations of CeO<sub>2</sub> NPs were inoculated with *S. aureus* and *P. aeruginosa* and left to incubate at 37°C for 72 h. When 72 h incubation was finished, the well plates were slowly drained and washed twice with distilled water. The plates were then

dried for 20 min at 70°C. After drying, crystal violet (CV) was added to stain biofilms for 30 min. CV was then removed and the plates were washed slowly. The washing step was done twice. Then ethanol was added, and waited 15 min for recovery of absorbed CV. The biofilm inhibition was determined by a spectrophotometer at 595 nm. Wells containing only *S. aureus* and *P. aeruginosa* with media were used as positive controls. Biofilm inhibition was calculated according to Equation (2).

$$\text{Biofilm Inhibition (\%)} = \left( \frac{\text{Abs}(\text{control}) - \text{Abs}(\text{sample})}{\text{Abs}(\text{control})} \right) \times 100 \quad (2)$$

## 2.7 | Statistical analysis

To assess the distribution normality, the Shapiro–Wilk test was selected. Data are represented as the median and 25th–75th percentile. Since seven groups of independent variables were analyzed, the Kruskal–Wallis and post hoc Dunn's tests were used. *P* values that do not exceed .05 indicated the statistically significant difference. All statistical calculations were performed by *GraphPad Prism* 5.0 software (USA).

## 2.8 | Bioethics

The study was performed in compliance with the EU Directive 2010/63/EU on the protection of animals. The study was approved by the Commission on Ethics and Bioethics (Kharkiv National Medical University, Kharkiv, Ukraine; minutes #3 dated August 28, 2020).

# 3 | RESULTS AND DISCUSSION

## 3.1 | Characterization of CeO<sub>2</sub> NPs

Transmission electron microscopy (TEM) images show that CeO<sub>2</sub> NPs obtained as described above were of about 2 and 10 nm size with a narrow size distribution (Figure 1A). Their crystal structure was confirmed by XRD analysis (Figure 1B). The XRD spectra of the solid phase of CeO<sub>2</sub> colloidal solutions match well to the standard diffraction data of FCC fluorite-type lattice (JCPDS card no. 34-0394). Citrate ions used for NPs stabilization imply the negative charge to the CeO<sub>2</sub> NPs surface:  $-12.75 \pm 0.92$  mV and  $-23.4 \pm 1.13$  mV for 2 and 10 nm CeO<sub>2</sub> NPs, respectively.

## 3.2 | Impact of CeO<sub>2</sub> nanoparticles on the eryptosis intensity

Eryptosis, that is, suicidal programmed cell death of erythrocytes, was assessed by annexin V staining. To evaluate its intensity quantitatively, two parameters were compared: the percentage of annexin V-positive erythrocytes, that is, those that display molecules of

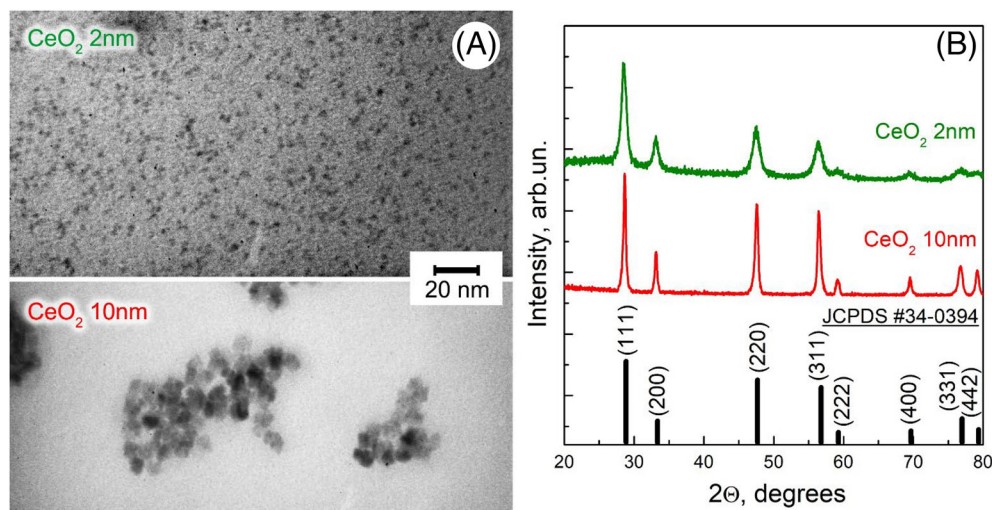


**FIGURE 1** Transmission electron microscopy (TEM) images (A) and X-ray diffraction spectra (XRD) pattern (B) of as-synthesized cerium oxide ( $\text{CeO}_2$ ) NPs.

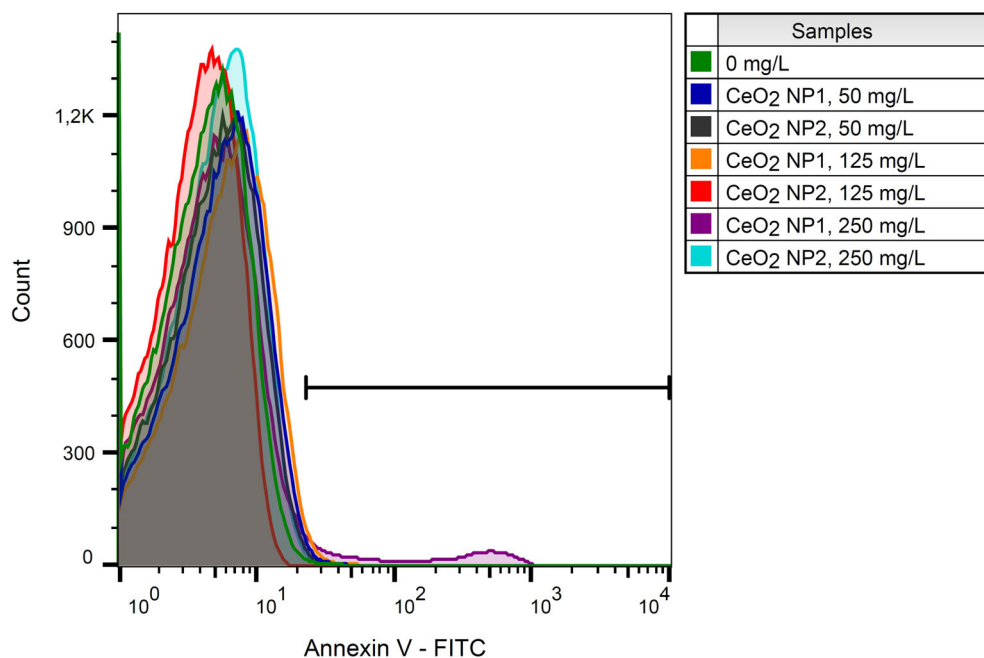


**FIGURE 2** Representative histograms of annexin V-FITC fluorescence. Erythrocytes exposed to various concentrations of cerium oxide ( $\text{CeO}_2$ ) nanoparticles were stained with annexin V-FITC for assessing eryptosis. Cerium oxide ( $\text{CeO}_2$ ) NP1 at a concentration of 250 mg/L were found to stimulate eryptosis.

phosphatidylserine on the surface, which is a sign of eryptosis, and the mean fluorescence intensity (MFI) of annexin V-FITC in all erythrocytes. Our findings are available in Figure 2 and Table 1. Both parameters were found to be statistically significantly higher only in the samples exposed to  $\text{CeO}_2$  NP1 at the highest used concentration, that is, 250 mg/L. The percentage of annexin V-stained cells was over 19-fold higher compared with the unexposed samples ( $p = .0039$ ). As for the MFI of annexin V-FITC in all erythrocytes, it was over 2.8-fold higher, respectively ( $p = .0015$ ). Thus, it can be assumed both  $\text{CeO}_2$  NP1 and  $\text{CeO}_2$  NP2 at concentrations of 125 mg/L. However, small-sized  $\text{CeO}_2$  nanoparticles induced eryptosis at a concentration of 250 mg/L.

Eryptosis is a rather novel assay for toxicity screening, which is suitable for nanoparticles as well.<sup>22–24</sup> This cell death mode of erythrocytes is characterized by cell shrinkage, blebbing and phosphatidylserine externalization, which can be detected using Annexin V

staining. Our findings indicate that smaller  $\text{CeO}_2$  NPs (1–2 nm) show cytotoxic properties promoting eryptosis, while the use of larger cerium oxide nanoparticles (10–12 nm) is safe at concentrations that do not exceed at least 250 mg/L. Thus, in this study, the cytotoxicity of nanoparticles against erythrocytes was found to be size-dependent. Our findings are consistent with the data obtained in other studies concerning cerium oxide nanoparticles. In particular, Ma et al. reported that the smallest nanoparticles are more toxic compared to the larger ones.<sup>25</sup>

### 3.3 | Antimicrobial activity

The antimicrobial activities of cerium nanoparticles synthesized in different sizes were investigated against eight pathogen microorganisms. These are microorganisms that are well known in medical

**TABLE 1** The percentage of annexin V-positive erythrocytes and mean fluorescence intensity values of annexin V-FITC were used to characterize the eryptosis intensity in erythrocytes exposed to cerium oxide nanoparticles (Me [IQR])

Samples	Percentage of annexin V-positive erythrocytes, %	P values	Mean fluorescence intensity of annexin V-FITC in erythrocytes, a.u.	P values
0 (mg/L)	0.60 (0.48; 1.03)		127 (124; 133)	
CeO <sub>2</sub> NP1 (50 mg/L)	0.85 (0.48; 1.35)	$p > .05$	125 (104; 160)	$p > .05$
CeO <sub>2</sub> NP2 (50 mg/L)	0.75 (0.65; 1.45)	$p > .05$	125 (118; 142)	$p > .05$
CeO <sub>2</sub> NP1 (125 mg/L)	1.20 (0.85; 1.93)	$p > .05$	156 (142; 187)	$p > .05$
CeO <sub>2</sub> NP2 (125 mg/L)	0.50 (0.48; 1.83)	$p > .05$	121 (110; 129)	$p > .05$
CeO <sub>2</sub> NP1 (250 mg/L)	11.45 (6.55; 28.18)	$p = .0039$	357 (239; 880)	$p = .0015$
CeO <sub>2</sub> NP2 (250 mg/L)	0.75 (0.48; 1.43)	$p > .05$	149 (108; 158)	$p > .05$

**TABLE 2** The minimum inhibition concentration (MIC) of test microorganisms.

Microorganisms	CeO <sub>2</sub> NP1	CeO <sub>2</sub> NP2
<i>E. coli</i>	128	128
<i>P. aeruginosa</i>	256	256
<i>L. pneumophila subsp. pneumophila</i>	256	256
<i>E. hirae</i>	128	128
<i>E. faecalis</i>	128	256
<i>S. aureus</i>	128	256
<i>C. parapsilosis</i>	256	256
<i>C. tropicalis</i>	256	256

Note: Numerical values are expressed in mg/L.

microbiology and cause serious infectious diseases in humans. The antimicrobial effects of cerium nanoparticles were analyzed using the microdilution method. The results are shown in Table 2. As seen in Table 2, both synthesized cerium nanoparticles showed antimicrobial activity against all test microorganisms. The MIC values were found to be 128 mg/L for *E. coli*, *E. hirae*, *E. faecalis*, and *S. aureus* and 256 mg/L for *P. aeruginosa*, *L. pneumophila subsp. pneumophila*, *C. parapsilosis*, and *C. tropicalis* when using a CeO<sub>2</sub> NP1. On the other hand, MIC values were determined to be 128 mg/L for *E. coli* and *E. hirae* and 256 mg/L for *E. faecalis*, *S. aureus*, *P. aeruginosa*, *L. pneumophila subsp. pneumophila*, *C. parapsilosis*, and *C. tropicalis* when CeO<sub>2</sub> NP2 was used. As the particle size decreased, the antimicrobial activity of the cerium nanoparticle against *E. faecalis* and *S. aureus* increased. It has been reported that cerium nanoparticles have the antimicrobial activity. In particular, Reshma and Ashwini investigated the antimicrobial activity of cerium nanoparticles against *E. coli*, *Proteus vulgaris*, *Corynebacterium diphtheriae*, and *Sarcinolutea*.<sup>26</sup> The synthesized cerium nanoparticles demonstrated antimicrobial activity against *E. coli* and *P. vulgaris* as well. Kannan and Sundrarajan synthesized and characterized cerium nanoparticles and studied their antimicrobial activity suggesting that the effectiveness of CeO<sub>2</sub> nanoparticles depends on their size and morphology.<sup>27</sup> These data are consistent with our findings.

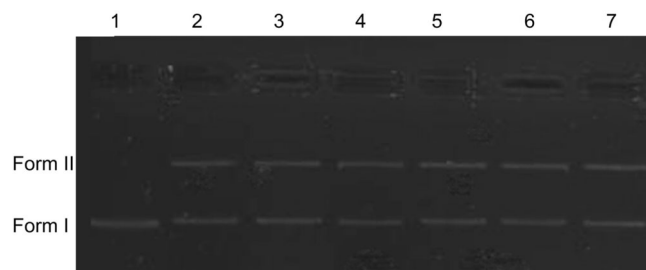
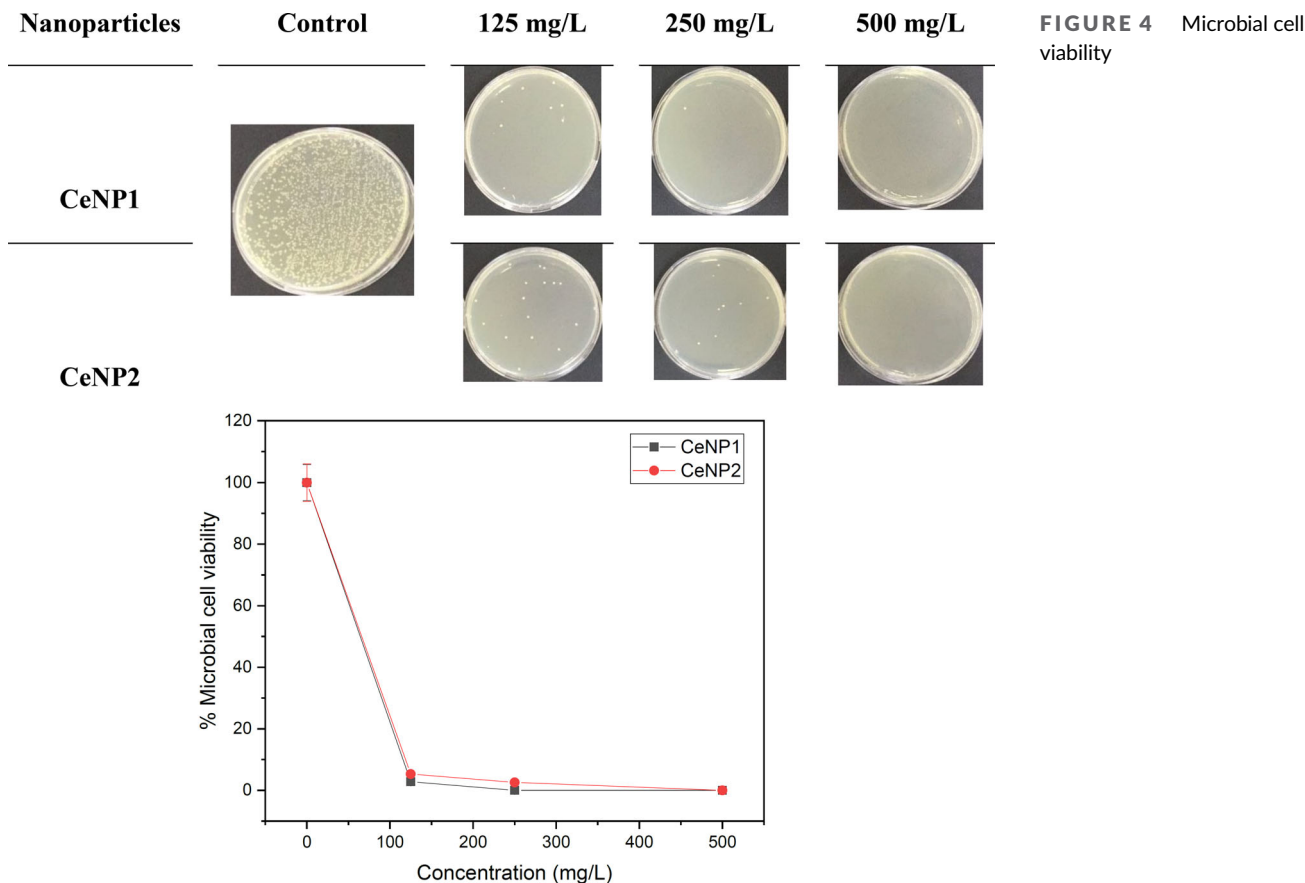


**FIGURE 3** DNA Cleavage activity of cerium oxide (CeO<sub>2</sub>) nanoparticles. (Lane 1) pBR 322 DNA, (Lane 2) pBR 322 DNA + 125 mg/L CeO<sub>2</sub> NP1, (Lane 3) pBR 322 DNA + 250 mg/L of CeO<sub>2</sub> NP1, (Lane 4) pBR 322 DNA + 500 mg/L of CeO<sub>2</sub> NP1, (Lane 5) pBR 322 DNA + 125 mg/L CeO<sub>2</sub> NP2, (Lane 6) pBR 322 DNA + 250 mg/L of CeO<sub>2</sub> NP2, (Lane 7) pBR 322 DNA + 500 mg/L of CeO<sub>2</sub> NP2.

### 3.4 | DNA cleavage activity

DNA cleavage analysis is a fast, simple, and reliable test to determine the effects of nanocomplexes on DNA under various conditions. The imaging method of this test was performed by agarose gel electrophoresis. The confirmation of the DNA bands after imaging allows interpreting the cleavage activity. Many cleavage agents interact with closed double-stranded DNA molecules, transforming supercoiled double-stranded DNA molecules from a superhelical form (Form I) to a broken form (Form II) and linear forms (Form III) and finally to small DNA fragments. The DNA cleavage activities of cerium oxide nanoparticles were tested by agarose gel electrophoresis using plasmid DNA. The effect of different concentrations of cerium oxide nanoparticles on DNA cleavage was investigated. The results are shown in Figure 3. As seen in Figure 3, CeO<sub>2</sub> NP1 and CeO<sub>2</sub> NP2 were shown to exhibit single-strand DNA cleavage activity at all tested concentrations. Nanozymes that include CeO<sub>2</sub> nanoparticles cause hydrolytic cleavage of single-stranded DNA oligonucleotides.<sup>28</sup> Xu et al. reported that CeO<sub>2</sub> nanoparticles and DNase I cleaved polyadenine DNA down to ~5-mer fragments as the major products, although further DNA cleavage to even shorter DNA fragments were obtained with CeO<sub>2</sub> nanoparticles.<sup>29</sup> Mittal and Pandey reported that cerium oxide nanoparticles caused reactive oxygen species (ROS) generation



in lung adenocarcinoma (A549) cells and an increase in oxidative DNA damage was observed as well.<sup>30</sup> Their study demonstrated that ROS-mediated DNA damage played a significant role in CeO<sub>2</sub> nanoparticles-induced apoptotic cell death in A549 cells. Our results showed good similarity with their findings.

### 3.5 | Microbial cell viability

The impact of synthesized and characterized CeO<sub>2</sub> NP1 and CeO<sub>2</sub> NP2 on microbial cell viability was investigated against *E. coli*. The results are represented in Figure 4. As seen in Figure 4, both types of CeO<sub>2</sub> NPs displayed an excellent microbial growth inhibition effect. When the concentration of synthesized CeO<sub>2</sub>NPs increased, it caused the internalization of more nanoparticles, thereby leading to the inhibition of microbial cells. CeO<sub>2</sub> NP1 was found to inhibit *E. coli* growth by 97.21%, 99.99%, and 100% at the concentrations of 125, 250, and 500 mg/L, respectively. On the other hand, CeO<sub>2</sub> NP2 exhibited 94.68%, 97.43%, and 100% bacterial growth inhibition at concentrations of 125, 250, and 500 mg/L, respectively. Similar results were observed by Nair et al. after utilizing ZnO nanoparticles.<sup>31</sup> Loo et al. reported that the tested bacteria were killed in a shorter time at lower concentrations of silver nanoparticles.<sup>32</sup> This may be due to the cell wall structure of Gram-negative bacteria. The cell wall characteristics of Gram-positive and Gram-negative bacteria show differences. In addition to these, nanoparticles can cause the formation of ROS in

cells. These ROS can show toxicity by attacking macromolecules such as proteins, enzymes, DNA, and so forth. Similar mechanisms may have occurred by cerium nanoparticles.

### 3.6 | Biofilm inhibition activity

The bacteria cause infectious diseases and these diseases are usually treated by antibiotics. The overuse and misuse of antibiotics have contributed to drug resistance in bacteria, and these events have become an important burden for the global health system.<sup>3</sup> Among the numerous proposed causes, bacterial biofilm formation was taken into account as a predominant factor in drug resistance development.<sup>33</sup> The biofilm has a complex functional and structural architecture consisting of proteins, extracellular DNA, and exopolysaccharides. It protects bacteria against antibiotics, as well as host defense.<sup>34</sup> Bacteria colonizing in a biofilm mode can cause persistent infection in the host, which is difficult to control, prevent, or eradicate. Therefore, there is a great demand for alternative antibacterial medicines with good biocompatibility and higher effectiveness.<sup>35,36</sup> In this study, the effects of CeO<sub>2</sub> NP1 and CeO<sub>2</sub> NP2 at different concentrations on biofilm inhibition of *P. aeruginosa* and *S. aureus* were studied. The result is shown in Figure 5. The biofilm inhibition activity was found to be concentration-dependent. Both synthesized CeO<sub>2</sub> NPs showed higher biofilm inhibition to *P. aeruginosa* than to *S. aureus*. When the concentration of CeO<sub>2</sub> NPs increased from 125 to 250 mg/L, the biofilm inhibition activity increased from 19.59%

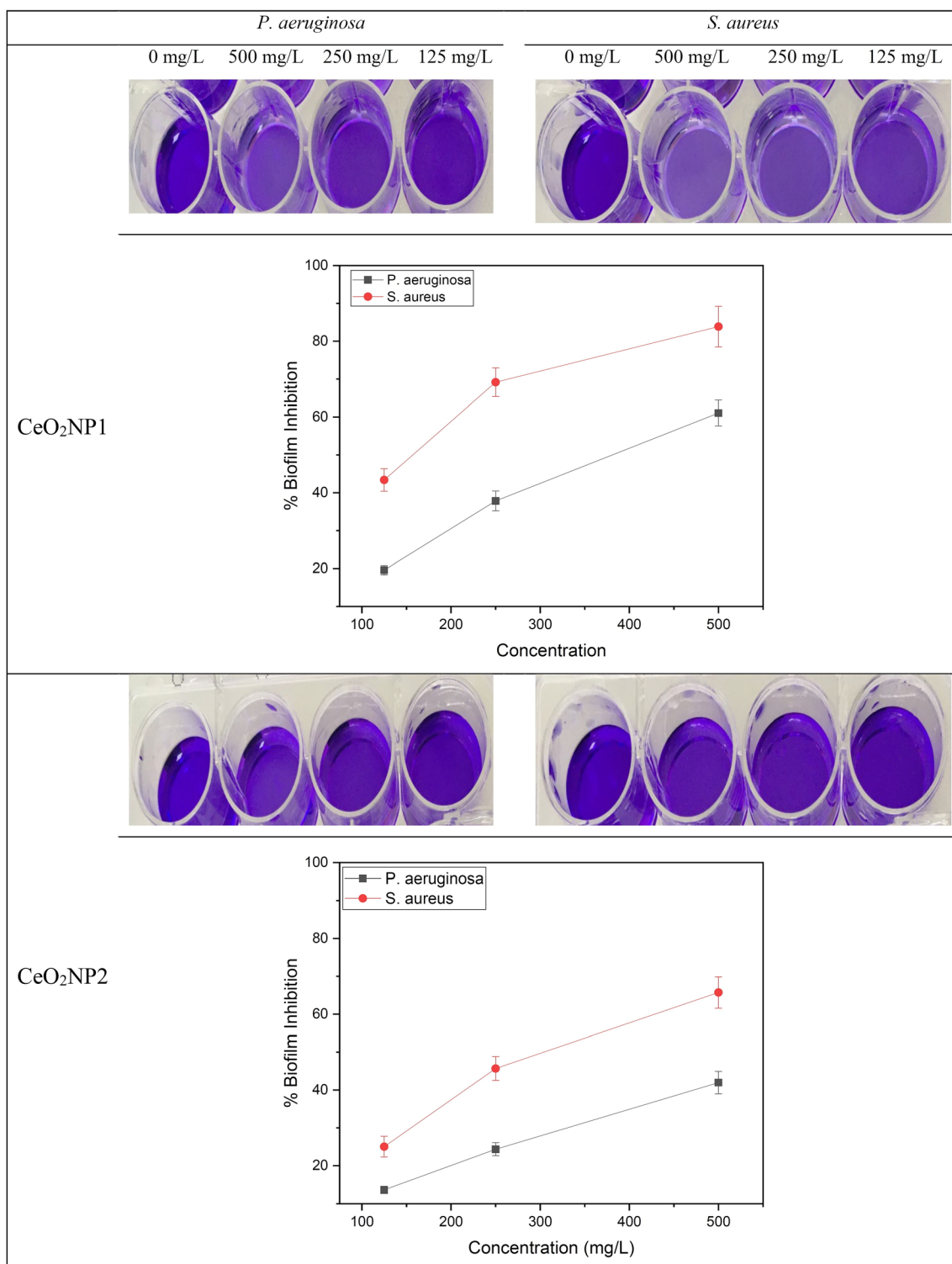


**FIGURE 5** Biofilm inhibition

to 37.84% for *P. aeruginosa* and from 43.39% to 69.16% for *S. aureus*. On the other hand, as the concentration of CeO<sub>2</sub> NP2 increased from 125 to 250 mg/L, the biofilm inhibition activities of *P. aeruginosa* and *S. aureus* were enhanced from 13.62% to 24.34% and from 25.03% to 45.68%, respectively. The highest biofilm inhibition activities were 61.06% for *P. aeruginosa* and 83.86% for

*S. aureus* when CeO<sub>2</sub> NP1 was used at a concentration of 500 mg/L. The inhibition mechanism of NPs on the formation of microbial biofilm can be related to ROS overproduction. It results in the development of oxidative stress, destruction of the bacterial cell wall. In addition, the released metal ions can bind to thiol groups of amino acid residues in proteins inactivating them.<sup>37</sup>

## 4 | CONCLUSION

The antioxidant and antimicrobial activity of synthesized CeO<sub>2</sub> nanoparticles were tested. CeO<sub>2</sub> nanoparticles show DNA cleavage activity when using plasmid DNA as a target DNA molecule. They significantly inhibit microbial cell viability against *E. coli*. In addition, the maximum biofilm inhibition abilities are obtained as 61.06% for *P. aeruginosa* and 83.86% for *S. aureus* using smaller CeO<sub>2</sub> nanoparticles (2 nm) at 500 mg/L. At the same time, larger nanoparticles are found to be less toxic against eukaryotic cells (erythrocytes). The results of our investigation show that the synthesized CeO<sub>2</sub> nanoparticles seem to be promising antimicrobial and anticancer agents.

### AUTHOR CONTRIBUTIONS

All authors have made substantial contributions to this article. Conceptualization: Nadir Dizge, Svetlana Yefimova, Anton Tkachenko; Data analysis & Original draft writing: Sadin Özdemir, Anton Tkachenko, Svetlana Yefimova, Anatolii Onishchenko; Experimental data acquisition: Serpil Gonca, Vladimir Klochkov, Nataliya Kavok, Anatolii Onishchenko; Interpretation of data: Serpil Gonca, Anatolii Onishchenko, Svetlana Yefimova, Anton Tkachenko; Statistical analysis: Kasim Ocakoglu, Tatyana Chumachenko, Vladimir Klochkov, Pavel Maksimchuk; Proofreading: Tatyana Chumachenko, Vladimir Klochkov, Nataliya Kavok; Funding: Tatyana Chumachenko, Nadir Dizge, Anton Tkachenko. All authors read and approved the final manuscript.

### FUNDING INFORMATION

The study was funded by the National Research Foundation of Ukraine in the framework of the research project no. 0120U105451 entitled "Development of Intelligent Technologies for Assessing the Epidemic Situation to Support Decision-Making in the Population Biosafety Management."

### CONFLICT OF INTEREST

The authors declare no conflicts of interest.

### DATA AVAILABILITY STATEMENT

Raw data were generated at Mersin University, Tarsus University and Kharkiv National Medical University. Derived data supporting the findings of this study are available from the corresponding author Anton Tkachenko on request.

### ORCID

Svetlana Yefimova  <https://orcid.org/0000-0003-2092-1950>  
 Vladimir Klochkov  <https://orcid.org/0000-0002-8080-1195>  
 Anton Tkachenko  <https://orcid.org/0000-0002-1029-1636>  
 Anatolii Onishchenko  <https://orcid.org/0000-0002-2122-2361>  
 Tatyana Chumachenko  <https://orcid.org/0000-0002-4175-2941>  
 Nadir Dizge  <https://orcid.org/0000-0002-7805-9315>  
 Sadin Özdemir  <https://orcid.org/0000-0002-8723-383X>  
 Serpil Gonca  <https://orcid.org/0000-0002-8544-1184>  
 Kasim Ocakoglu  <https://orcid.org/0000-0003-2807-0425>

## REFERENCES

- Manyi-Loh C, Mamphweli S, Meyer E, Okoh A. Antibiotic use in agriculture and its consequential resistance in environmental sources: potential public health implications. *Molecules*. 2018;23(4):795. doi:10.3390/molecules23040795
- Landers TF, Cohen B, Wittum TE, Larson EL. A review of antibiotic use in food animals: perspective, policy, and potential. *Public Health Rep*. 2012;127(1):4-22. doi:10.1177/003335491212700103
- Ventola CL. The antibiotic resistance crisis: part 1: causes and threats. *Pharm Therapeut*. 2015;40(4):277-283.
- Piewngam P, Chiou J, Chatterjee P, Otto M. Alternative approaches to treat bacterial infections: targeting quorum-sensing. *Expert Rev Anti Infect Ther*. 2020;18(6):499-510. doi:10.1080/14787210.2020.1750951
- Lei J, Sun L, Huang S, et al. The antimicrobial peptides and their potential clinical applications. *Am J Transl Res*. 2019;11(7):3919-3931.
- Romero-Calle D, Guimarães Benevides R, Góes-Neto A, Billington C. Bacteriophages as alternatives to antibiotics in clinical care. *Antibiotics (Basel)*. 2019;8(3):138. doi:10.3390/antibiotics8030138
- Mahlapuu M, Håkansson J, Ringstad L, Björn C. Antimicrobial peptides: an emerging category of therapeutic agents. *Front Cell Infect Microbiol*. 2016;6:194. doi:10.3389/fcimb.2016.00194
- Loc-Carrillo C, Abedon ST. Pros and cons of phage therapy. *Bacteriophage*. 2011;1(2):111-114. doi:10.4161/bact.1.2.14590
- Amaro F, Morón Á, Díaz S, Martín-González A, Gutiérrez JC. Metallic nanoparticles-friends or foes in the battle against antibiotic-resistant bacteria? *Microorganisms*. 2021;9(2):364. doi:10.3390/microorganisms9020364
- Lee NY, Ko WC, Hsueh PR. Nanoparticles in the treatment of infections caused by multidrug-resistant organisms. *Front Pharmacol*. 2019;10:1153. doi:10.3389/fphar.2019.01153
- Slavin YN, Asnis J, Häfeli UO, Bach H. Metal nanoparticles: understanding the mechanisms behind antibacterial activity. *J Nanobiotechnol*. 2017;15(1):65. doi:10.1186/s12951-017-0308-z
- McNeilly O, Mann R, Hamidian M, Gunawan C. Emerging concern for silver nanoparticle resistance in *Acinetobacter baumannii* and other bacteria. *Front Microbiol*. 2021;12:652863. doi:10.3389/fmicb.2021.652863
- Niño-Martínez N, Salas Orozco MF, Martínez-Castañón GA, Torres Méndez F, Ruiz F. Molecular mechanisms of bacterial resistance to metal and metal oxide nanoparticles. *Int J Mol Sci*. 2019;20(11):2808. doi:10.3390/ijms20112808
- Panáček A, Kvítek L, Směkalová M, et al. Bacterial resistance to silver nanoparticles and how to overcome it. *Nat Nanotechnol*. 2018;13(1):65-71. doi:10.1038/s41565-017-0013-y
- Sánchez-López E, Gomes D, Esteruelas G, et al. Metal-based nanoparticles as antimicrobial agents: an overview. *Nanomaterials (Basel)*. 2020;10(2):292. doi:10.3390/nano10020292
- Wang L, Hu C, Shao L. The antimicrobial activity of nanoparticles: present situation and prospects for the future. *Int J Nanomed*. 2017;12:1227-1249. doi:10.2147/IJN.S121956
- Pop OL, Mesaros A, Vodnar DC, et al. Cerium oxide nanoparticles and their efficient antibacterial application in vitro against gram-positive and gram-negative pathogens. *Nanomaterials (Basel)*. 2020;10(8):1614. doi:10.3390/nano10081614
- Farias IAP, Dos Santos CCL, Sampaio FC. Antimicrobial activity of cerium oxide nanoparticles on opportunistic microorganisms: a systematic review. *Biomed Res Int*. 2018;2018:1923606-1923614. doi:10.1155/2018/1923606
- Alpaslan E, Geilich BM, Yazici H, Webster TJ. pH-controlled cerium oxide nanoparticle inhibition of both gram-positive and gram-negative bacteria growth. *Sci Rep*. 2017;7:45859. doi:10.1038/srep45859



20. Dong Y, Zhu H, Shen Y, Zhang W, Zhang L. Antibacterial activity of silver nanoparticles of different particle size against vibrio natriegens. *PLoS One*. 2019;14(9):e0222322. doi:[10.1371/journal.pone.0222322](https://doi.org/10.1371/journal.pone.0222322)
21. Klochkov VK, Grigorova AV, Sedyh OO, Malyukin YV. The influence of agglomeration of nanoparticles on their SOD mimetic activity. *Colloids Surf A: Physicochem Eng Aspects*. 2012;409:176-182.
22. Ran Q, Xiang Y, Liu Y, et al. Eryptosis indices as a novel predictive parameter for biocompatibility of Fe<sub>3</sub>O<sub>4</sub> magnetic nanoparticles on erythrocytes. *Sci Rep*. 2015;5:16209. doi:[10.1038/srep16209](https://doi.org/10.1038/srep16209)
23. Onishchenko A, Myasoedov V, Yefimova S, et al. UV light-activated GdYVO<sub>4</sub>:Eu<sup>3+</sup> nanoparticles induce reactive oxygen species generation in leukocytes without affecting erythrocytes In vitro. *Biol Trace Elem Res*. 2022;200(6):2777-2792. doi:[10.1007/s12011-021-02867-z](https://doi.org/10.1007/s12011-021-02867-z)
24. Tkachenko A, Kot Y, Prokopyuk V, et al. Food additive E407a stimulates eryptosis in a dose-dependent manner. *Wien Med Wochenschr*. 2022;172:135-143. doi:[10.1007/s10354-021-00874-2](https://doi.org/10.1007/s10354-021-00874-2)
25. Ma Y, Li P, Zhao L, et al. Size-dependent cytotoxicity and reactive oxygen species of cerium oxide nanoparticles in human retinal pigment epithelia cells. *Int J Nanomedicine*. 2021;16:5333-5341. doi:[10.2147/IJN.S305676](https://doi.org/10.2147/IJN.S305676)
26. Reshma P, Ashwini K. Cerium oxide nanoparticles: synthesis, characterization and study of antimicrobial activity. *J Nanomater Mol Nanotechnol*. 2017;06(3):2-6. doi:[10.4172/2324-8777.1000219](https://doi.org/10.4172/2324-8777.1000219)
27. Kannan S, Sundrarajan M. A green approach for the synthesis of a cerium oxide nanoparticle: characterization and antibacterial activity. *Int J Nanosci*. 2014;13(3):1450018. doi:[10.1142/S0219581X14500185](https://doi.org/10.1142/S0219581X14500185)
28. Fang R, Liu J. Cleaving DNA by nanozymes. *J Mater Chem B*. 2020;8:7135-7142.
29. Xu F, Lu Q, Huang PJ, Liu J. Nanoceria as a DNase I mimicking nanozyme. *Chem Commun (Camb)*. 2019;55(88):13215-13218. doi:[10.1039/c9cc06782e](https://doi.org/10.1039/c9cc06782e)
30. Mittal S, Pandey AK. Cerium oxide nanoparticles induced toxicity in human lung cells: role of ROS mediated DNA damage and apoptosis. *Biomed Res Int*. 2014;2014:891934. doi:[10.1155/2014/891934](https://doi.org/10.1155/2014/891934)
31. Nair S, Sasidharan A, Divya Rani VV, et al. Role of size scale of ZnO nanoparticles and microparticles on toxicity toward bacteria and osteoblast cancer cells. *J Mater Sci Mater Med Suppl*. 2009;1:S235-S241. doi:[10.1007/s10856-008-3548-5](https://doi.org/10.1007/s10856-008-3548-5)
32. Loo YY, Rukayadi Y, Nor-Khaizura MA, et al. In vitro antimicrobial activity of green synthesized silver nanoparticles against selected gram-negative foodborne pathogens. *Front Microbiol*. 2018;9:1555. doi:[10.3389/fmicb.2018.01555](https://doi.org/10.3389/fmicb.2018.01555)
33. Høiby N, Bjørnsholt T, Givskov M, Molin S, Ciofu O. Antibiotic resistance of bacterial biofilms. *Int J Antimicrob Agents*. 2010;35(4):322-332. doi:[10.1016/j.ijantimicag.2009.12.011](https://doi.org/10.1016/j.ijantimicag.2009.12.011)
34. Roilides E, Simitsopoulou M, Katragkou A, Walsh TJ. How biofilms evade host defenses. *Microbiol Spectr*. 2015;3(3). doi:[10.1128/microbiolspec.MB-0012-2014](https://doi.org/10.1128/microbiolspec.MB-0012-2014)
35. Subramaniyan SB, Megarajan S, Dharshini KS, Veerappan A. Artocarpus integrifolia seed lectin enhances membrane damage, oxidative stress and biofilm inhibition activity of silver nanoparticles against *Staphylococcus aureus*. *Colloids Surf A Physicochem Eng Asp*. 2021;624:126842.
36. Xu J, Li Y, Wang H, Zhu M, Feng W, Liang G. Enhanced antibacterial and anti-biofilm activities of antimicrobial peptides modified silver nanoparticles. *Int J Nanomedicine*. 2021;16:4831-4846. doi:[10.2147/IJN.S315839](https://doi.org/10.2147/IJN.S315839)
37. Shkodenko L, Kassirov I, Koshel E. Metal oxide nanoparticles against bacterial biofilms: perspectives and limitations. *Microorganisms*. 2020;8(10):1545. doi:[10.3390/microorganisms8101545](https://doi.org/10.3390/microorganisms8101545)

**How to cite this article:** Yefimova S, Klochkov V, Kavok N, et al. Antimicrobial activity and cytotoxicity study of cerium oxide nanoparticles with two different sizes. *J Biomed Mater Res*. 2022;1-9. doi:[10.1002/jbm.b.35197](https://doi.org/10.1002/jbm.b.35197)